

C-MIG: Multi-view Information Gain-based Retrieval-Augmented Generation for Clinical Diagnosis Reasoning

Yuwei Miao^{1,*}, Gen Li^{1,*}, Yunsheng Zeng^{1,*}, Xiandong Li¹, Yujin Wang¹, Siyu Chen¹,
Luning Wang¹, Yunhao Qiao¹, Junfeng Wang¹, Jianwei Lv^{1,†}, Bo Yuan^{1,†}
¹Baidu Inc.

Abstract

Retrieval-augmented generation combined with reinforcement learning has shown promise for grounding large language models in trustworthy medical evidence. However, existing methods rely on exact-match binary rewards, which in clinical diagnosis cause two issues: (i) semantically relevant but non-verbatim steps receive zero signal, discarding valuable learning signals; and (ii) uni-dimensional rewards cannot effectively supervise heterogeneous reasoning capabilities. To address these issues, we propose **C-MIG**, a **M**ulti-view **I**nformation **G**ain-based retrieval-augmented generation framework for **C**linical diagnosis. C-MIG estimates information gain under a frozen reference model from two complementary views, retrieved-document and document-refinement, to jointly guide *what to retrieve* and *how to refine*, alleviating the issues of valuable reward signal loss and credit assignment. We further design a multi-subquery retrieval augmentation strategy that improves knowledge recall coverage in clinical diagnostic scenarios. Comprehensive experiments on four medical benchmarks demonstrate that C-MIG achieves the best performance among all RAG-RL methods on both in-domain and out-of-domain sets, and outperforms state-of-the-art general-purpose LLMs for clinical diagnosis.

1 Introduction

Large language models (LLMs) have been increasingly applied to clinical diagnosis (Dou et al., 2025; Qiu et al., 2025; Liao et al., 2025), aiming to provide efficient and accurate responses to patient queries. However, outdated knowledge, insufficient domain specialization, and the limitations of parametric memorization cause LLMs to hallucinate

* Equal contribution.
miaoyuwei25@mails.ucas.ac.cn

† Corresponding author.
{yuanbo07,lvjianwei}@baidu.com

E-mail:

E-mail:

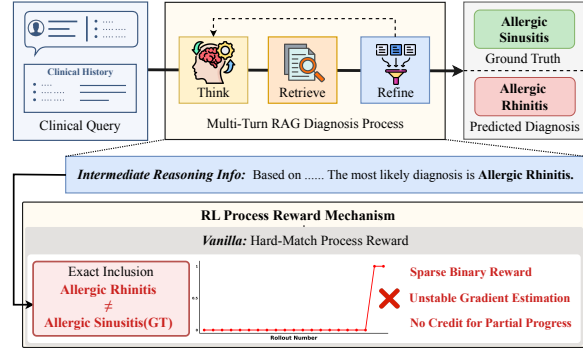


Figure 1: Hard process rewards assign zero signal to semantically relevant intermediate steps, causing reward sparsity and suboptimal credit assignment.

nate (Orgad et al., 2025; Huang et al., 2025; Feng et al., 2026), posing direct risks to patient safety.

Retrieval-augmented generation (RAG) (Li et al., 2025b; Wang et al., 2026a) has emerged as a mainstream solution to mitigate LLM hallucinations by dynamically integrating external knowledge into the generation process, improving factual reliability. Recent studies (Jin et al., 2025; Zhao et al., 2025; Song et al., 2025; Wang et al., 2025a; Shi et al., 2026; Wang et al., 2026b) have drawn inspiration from reinforcement learning (RL) and explored applying RAG to RL reasoning tasks, achieving promising results by evaluating only the correctness of final answers.

Despite their effectiveness, existing RAG-RL methods (Zhao et al., 2025; Song et al., 2025; Shi et al., 2026) typically rely on exact matching to provide binary (0/1) rewards. As shown in Figure 1, even when intermediate reasoning correctly identifies a clinically relevant diagnosis, both outcome and hard process rewards (e.g., exact inclusion in AutoRefine (Shi et al., 2026)) yield zero because the output does not verbatim match the ground truth. This exposes two limitations in clinical diagnosis:

Hard process rewards discard valuable medical signals: Medical nomenclature exhibits inher-

ent semantic similarity (e.g., “Allergic Sinusitis” vs. “Allergic Rhinitis”). While exact matching remains necessary for final outcome evaluation, intermediate reasoning steps that surface clinically relevant information still deserve meaningful credit. Hard process rewards inherit exact-matching brittleness, assigning zero signal to such informative steps that do not contain the ground truth verbatim.

Uni-dimensional signals lack multi-capability supervision: Current process rewards target a single dimension—either retrieval or summarization—without jointly providing multi-granularity supervision, resulting in suboptimal credit assignment across heterogeneous reasoning steps.

Concurrent work IGPO (Wang et al., 2025a) introduces turn-level information gain as process rewards. However, it is tailored for multi-hop QA and computes information gain between consecutive turns’ overall outputs; in medical consultation where models sometimes converge to single-turn retrieval, such inter-turn differentials become uninformative. Moreover, IGPO provides only a single-view reward signal and computes posteriors with the continuously updated policy model, leading to reward drift as training progresses.

To address the above limitations, we propose **C-MIG**, a **Multi-view Information Gain**-based retrieval-augmented generation framework for **Clinical diagnosis**. C-MIG formulates information gain as a unified process reward that captures two complementary aspects: (1) the incremental benefit of newly retrieved documents over the previous turn’s retrieval, and (2) the contribution of the model’s refined summary relative to the raw query alone. These two signals synergistically supervise “what to retrieve” and “how to refine.” A frozen reference model is employed for all reward computations, fundamentally eliminating reward drift. We further introduce a multi-subquery strategy to improve knowledge recall under ambiguous patient inquiries. Experiments on four medical benchmarks demonstrate that C-MIG surpasses IGPO by 6.71 points in-domain and achieves the best out-of-domain generalization.

Our contributions are summarized as follows:

- We propose C-MIG, a multi-view information gain framework that employs a frozen reference model to compute process rewards, quantifying the importance of individual reasoning steps while eliminating reward drift caused by policy distribution shift.

- We design two complementary reward views—document-level retrieval gain and refinement-level summarization gain—that jointly improve retrieval and summarization capabilities. The mechanism is extensible, requires no additional reward model, and introduces minimal computational overhead.
- We introduce a multi-subquery retrieval strategy to improve knowledge recall under ambiguous inputs. Experiments on four medical benchmarks show that C-MIG achieves state-of-the-art performance, providing a generalizable RAG-RL solution for clinical diagnosis.

2 Method

The framework of C-MIG is shown in Figure 2. C-MIG, grounded in the joint framework of RAG and RL, decomposes colloquial patient inquiries into semantically complementary, medically standardized subqueries. It employs a frozen reference model to compute information gain from two perspectives: the retrieved document level and the document refinement level, quantifying the importance of individual reasoning steps and synergistically guiding the model to continuously align with clinical diagnostic goals across the two dimensions of “what to retrieve” and “how to refine”. This section will describe C-MIG in detail.

2.1 Rollout Generation

Task Formulation Given a clinical query q and its diagnostic label a , the policy model π_θ generates a rollout through multi-turn interaction with a retrieval engine \mathcal{E} . Each round comprises four structured operations: `<think>` for analyzing patient query information and planning retrieval directions, `<search>` for issuing queries to the retrieval engine, `<evidence>` for receiving documents returned by the retrieval, `<refine>` for filtering and summarizing the retrieved documents. After several think-search-refine cycles, the model outputs conclusion in `<diagnosis>` tags. The number of cycles is determined autonomously, and the generation process terminates either upon producing a diagnosis or upon reaching the maximum allowed cycles number T_{\max} .

Multi-Subquery Generation and Retrieval In clinical diagnosis, patient inquiries are often colloquial and incomplete. Unlike conventional retrieval that returns top- k documents from a single

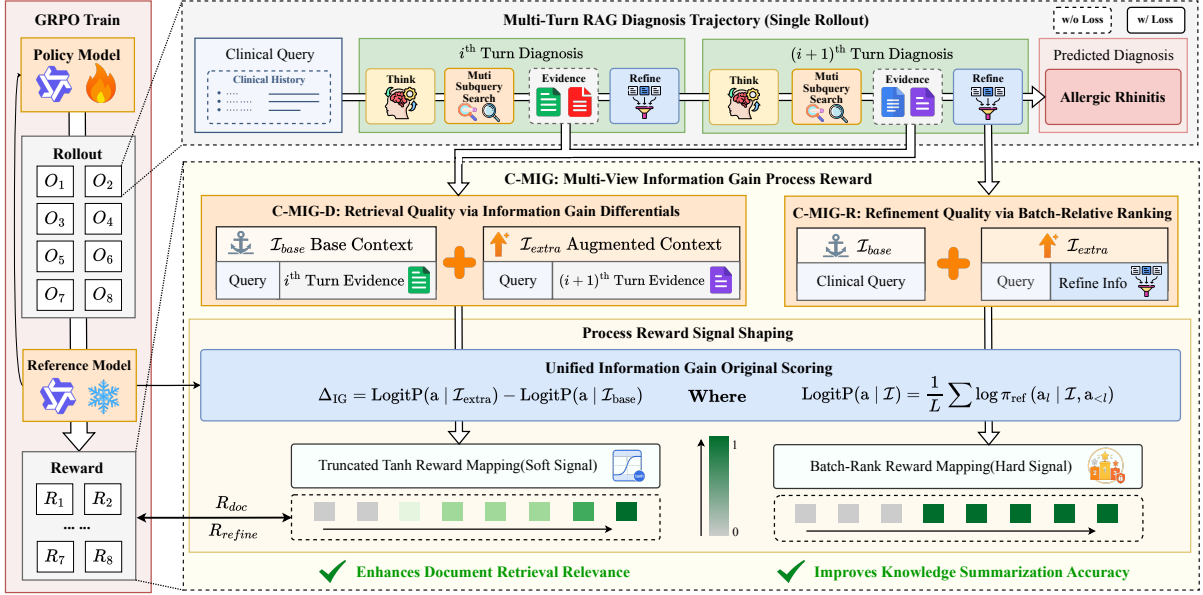


Figure 2: Overview of C-MIG. The framework integrates multi-turn RAG trajectory generation with multi-view information gain process rewards shaped via truncated tanh (soft signal) and batch-rank (hard signal) mappings.

query, we prompt the model to generate k semantically complementary subqueries, each retrieving the single most relevant document. The k retrieved documents are enclosed within `<evidence>`. The subquery generation is guided by task-specific prompts.

Following AutoRefine (Shi et al., 2026), we prompt the model to summarize and refine these documents, extracting critical information and filtering noise. The refined knowledge is placed within `<refine>`. Complete prompts are provided in Appendix A.

2.2 Multi-View Information Gain

As discussed in §1, hard process rewards based on exact string matching assign zero signal to semantically relevant but non-verbatim intermediate steps, causing reward sparsity for clinically informative outputs. We propose a multi-view information gain method to provide continuous reward signals: if the retrieval or refinement process facilitates diagnosis, the reference model’s predictive confidence in the correct answer should increase; otherwise, it should decrease.

Formally, given a frozen base model π_{ref} (not updated during training) and the gold answer $a = (a_1, \dots, a_L)$ of length L , we define the log-probability scoring function:

$$\text{LogitP}(a | \mathcal{I}) = \frac{1}{L} \sum_{l=1}^L \log \pi_{\text{ref}}(a_l | \mathcal{I}, a_{<l}) \quad (1)$$

where \mathcal{I} denotes the contextual information provided to the reference model. Based on this, we define the unified information gain as:

$$\Delta_{\text{IG}} = \text{LogitP}(a | \mathcal{I}_{\text{extra}}) - \text{LogitP}(a | \mathcal{I}_{\text{base}}) \quad (2)$$

where $\mathcal{I}_{\text{base}}$ is the base context before incorporating new information, and $\mathcal{I}_{\text{extra}}$ is the augmented context after incorporating the intermediate output (retrieved documents or refined knowledge). $\Delta_{\text{IG}} > 0$ indicates that the new information reduces diagnostic uncertainty, while $\Delta_{\text{IG}} \leq 0$ indicates noise introduction.

Distribution Shift Avoidance. All posteriors are computed by the frozen π_{ref} , not the continuously updated π_{θ} . Wang et al. (2025a) uses the policy model for posterior computation, suffering from reward drift as the policy distribution shifts during training. Our frozen π_{ref} provides a time-invariant anchor, guaranteeing reward consistency throughout training.

We instantiate Eq. 2 from two complementary views to address the credit assignment problem: C-MIG-D (§2.2.1) evaluates cross-turn retrieval quality by measuring information gain between successive retrieval rounds, and C-MIG-R (§2.2.2) evaluates intra-turn refinement quality by measuring the information gain of knowledge summarization.

2.2.1 C-MIG-D: Retrieval Quality via Information Gain Differentials

C-MIG-D progressively incentivizes the model to retrieve more valuable documents by measuring cross-turn information gain. For a trajectory with N rounds, we instantiate Eq. 2 by setting $\mathcal{I}_{\text{base}} = (q, D_{k-1})$ and $\mathcal{I}_{\text{extra}} = (q, D_k)$, where D_k denotes the documents returned in round k . The information gain is:

$$\Delta(D_k) = \text{LogitP}(a | q, D_k) - \text{LogitP}(a | q, D_{k-1}) \quad (3)$$

Inter-round improvement is measured by:

$$\delta_k = \Delta(D_k) - \Delta(D_{k-1}), \quad k = 2, \dots, N \quad (4)$$

To avoid introducing noise, we add two constraints: (1) First-Round Quality Gate: C-MIG-D reward is zero if $\Delta(D_1) \leq 0$, preventing reward hacking where the model deliberately performs ineffective first-round retrieval to inflate subsequent information gain, (2) Half-Positive Scheme, that truncates negative δ_k to zero. The combined reward is mapped via a truncated tanh function:

$$R_{\text{doc}} = \begin{cases} 0, & \Delta(D_1) \leq 0 \text{ or } N < 2 \\ \frac{w_d}{N} \sum_{k=2}^N \max(\tanh(\alpha_d \delta_k), 0), & \text{otherwise} \end{cases} \quad (5)$$

where α_d is a sensitivity parameter and w_d is a weight coefficient.

2.2.2 C-MIG-R: Refinement Quality via Batch-Relative Ranking

C-MIG-R measures the actual contribution of the refined content to diagnostic confidence by measuring intra-turn information gain. We instantiate Eq. 2 by setting $\mathcal{I}_{\text{base}} = q$ and $\mathcal{I}_{\text{extra}} = (q, s_{\text{refine}})$, where s_{refine} is the generated refinement. The information gain is:

$$\Delta(s_{\text{refine}}) = \text{LogitP}(a | q, s_{\text{refine}}) - \text{LogitP}(a | q) \quad (6)$$

where $\Delta(s_{\text{refine}}) > 0$ indicates effective extraction of diagnostic-relevant information, and $\Delta(s_{\text{refine}}) \leq 0$ indicates failure to provide incremental knowledge.

Unlike C-MIG-D, where verbose external documents yield continuously varying gain magnitudes suited to truncated tanh mapping, refinement is model-generated and concise, making absolute magnitude less informative than relative

standing within a batch. We therefore convert $\Delta(s_{\text{refine}})$ into rewards using a batch-rank reward mapping strategy. Within each batch, we compute the median $\tilde{\Delta}^+$ over all positive-gain samples $\mathcal{P} = \{i : \Delta(s_{\text{refine}})^{(i)} > 0\}$ and reward only the upper half:

$$R_{\text{refine}}^{(i)} = \begin{cases} w_r, & \text{if } \Delta(s_{\text{refine}})^{(i)} \geq \tilde{\Delta}^+ > 0 \\ 0, & \text{otherwise} \end{cases} \quad (7)$$

where $\tilde{\Delta}^+ = \text{median}(\{\Delta(s_{\text{refine}})^{(i)}\}_{i \in \mathcal{P}})$. This design dynamically adjusts the threshold according to batch difficulty, thereby avoiding over-incentivizing low-quality refinement.

C-MIG-D and C-MIG-R synergistically guide “what to retrieve” and “how to refine,” jointly aligning the model toward the diagnostic objective.

2.3 Outcome Rewards and Training Objective

We introduce two outcome rewards: format reward and diagnosis reward.

Format Reward. R_{format} is used to ensure that the model outputs in the correct format, i.e., all tags are correct and the number of <evidence> tags does not exceed the number of <search> tags. If the output format is correct, then $R_{\text{format}} = w_f$, otherwise, $R_{\text{format}} = 0$.

Diagnostic Reward. R_{diag} applies exact matching on normalized text within <diagnosis> tags: match yields 1, otherwise 0.

The overall reward is as follows:

$$R_{\text{total}} = R_{\text{format}} + R_{\text{diag}} + R_{\text{doc}} + R_{\text{refine}} \quad (8)$$

Policy Optimization. We adopt Group Relative Policy Optimization (GRPO) (Guo et al., 2025). For each sample (q, a) , we sample G trajectories $\{o_i\}_{i=1}^G$. Let $r_t(\theta) = \frac{\pi_\theta(o_{i,t}|q, o_{i,<t})}{\pi_{\theta_{\text{old}}}(o_{i,t}|q, o_{i,<t})}$ denote the importance ratio. The objective is:

$$\mathcal{J}(\theta) = \mathbb{E} \left[\frac{1}{G} \sum_{i=1}^G \frac{1}{|o_i|} \sum_{t=1}^{|o_i|} \min(r_t \hat{A}_{i,t}, \text{clip}(r_t, 1-\epsilon, 1+\epsilon) \hat{A}_{i,t}) - \beta D_{\text{KL}}[\pi_\theta \| \pi_{\text{ref}}] \right] \quad (9)$$

Advantages are estimated via group z-score normalization:

$$\hat{A}_i = \frac{R_i - \text{mean}(\{R_j\}_{j=1}^G)}{\text{std}(\{R_j\}_{j=1}^G) + \epsilon} \quad (10)$$

Tokens within <evidence> tags are masked during loss computation, as they are environment-generated and should not receive policy gradients.

Methods	MedDDx-Plus (In)			MedQA (OOD)			MedXpertQA (OOD)			RJUA (OOD)			Overall Avg
	EM	KG	Avg	EM	KG	Avg	EM	KG	Avg	EM	KG	Avg	
<i>Base Model</i>													
Qwen2.5-3B	0.30	0.30	0.30	0.50	1.00	0.75	0.79	2.57	1.68	0.00	1.23	0.61	0.84
<i>LLMs</i>													
Huatuogpt2-13B	1.10	2.53	1.81	0.50	1.80	1.15	1.19	4.28	2.73	1.90	3.41	2.65	2.09
Baichuan2-13B-Chat	3.69	11.41	7.55	2.50	6.60	4.55	1.19	3.01	2.10	12.32	22.46	17.39	7.90
Llama3-Med42-70B	8.87	20.40	14.64	7.50	19.90	13.70	3.37	7.56	5.47	9.00	13.36	11.18	11.25
DeepSeek-V4-Pro	21.93	43.11	32.52	20.00	29.20	24.60	22.97	24.63	23.80	9.48	24.55	17.01	24.48
GPT-5.2	20.04	42.85	31.45	12.00	25.20	18.60	8.12	13.31	10.71	8.53	31.94	20.24	20.25
<i>RAG+RL Methods</i>													
Search-R1	54.34	57.61	55.98	3.50	11.90	7.70	0.99	1.82	1.41	7.11	19.53	13.32	19.60
AutoRefine	48.65	51.47	50.06	7.00	12.00	9.50	3.96	8.51	6.23	8.53	24.35	16.44	20.56
IGPO	51.84	54.58	53.21	7.00	13.10	10.05	5.54	11.01	8.28	8.53	25.97	17.25	22.20
<i>Clinical Sparse Reward Methods</i>													
AutoRefine-Embedding	52.14	61.44	56.79	6.00	11.90	8.95	3.76	8.95	6.35	12.80	24.46	18.63	22.68
AutoRefine-ICDTree	43.87	64.09	53.98	3.00	12.60	7.80	6.14	13.74	9.94	13.27	24.27	18.77	22.62
AutoRefine-HardSearch	48.75	52.50	50.62	5.50	13.80	9.65	6.73	12.12	9.43	10.43	24.45	17.44	21.79
AutoRefine-HardDoc	52.94	58.52	55.73	5.50	11.40	8.45	4.36	7.52	5.94	7.11	18.77	12.94	20.77
C-MIG	57.43	62.41	59.92	6.50	15.20	10.85	7.33	12.08	9.71	9.95	26.82	18.38	24.72

Table 1: Performance on the in-domain dataset MedDDx-Plus and three out-of-domain datasets: MedQA, MedXpertQA, RJUA.

3 Experiments and Results

3.1 Experimental Settings

We conduct experiments using two types of models: Qwen-2.5-3B and Qwen-2.5-7B (Qwen et al., 2025) as the backbone and the following methods as baseline: **Base Model**: directly inference without any training. **Search-R1** (Jin et al., 2025): use EM rewards for multi-round retrieval and reasoning. **AutoRefine** (Shi et al., 2026): Extends Search-R1 by incorporating a knowledge refinement step and rewarding the quality of refined content. **IGPO** (Wang et al., 2025a): Employs the policy model itself to compute turn-level information gain as a process reward.

Additionally, we extend AutoRefine (Shi et al., 2026) to address the sparse reward problem in clinical diagnosis, where semantically equivalent disease names (e.g., synonyms or hierarchical variants) receive zero reward under exact matching. We design two soft outcome reward variants: **AutoRefine-Embedding**: replaces EM with embedding-based semantic similarity as the diagnostic reward. **AutoRefine-ICDTree**: computes a hierarchical soft reward based on node distance in the ICD (Maercker et al., 2013) disease taxonomy. We also design two hard process reward variants to enhance retrieval quality: **AutoRefine-HardSearch**: assigns a binary (0/1) reward based on whether the generated search queries contain the ground-truth diagnosis. **AutoRefine-HardDoc**: assigns a binary (0/1) reward based on whether the retrieved documents contain the ground-truth diagnosis.

We further select three medical large language models, **Huatuogpt2-13B** (Chen et al., 2023), **Baichuan2-13B-Chat** (Baichuan, 2023), and **Llama3-Med42-70B** (Christophe et al., 2024), together with two state-of-the-art general-purpose large language models, **DeepSeek-V4-Pro** (DeepSeek-AI, 2026) and **GPT-5.2**¹, for comparison. The hyperparameter configurations, datasets, and evaluation protocols are detailed in Appendix B.

3.2 Main Results

3.2.1 Overall Performance

Table 1 compares the clinical diagnostic performance of C-MIG against baselines on Qwen2.5-3B (Qwen2.5-7B results are in Appendix C), yielding the following observations:

Process rewards derived from posterior probability changes exhibit stronger robustness and generalizability. Under the same backbone and training protocol, C-MIG consistently outperforms all RAG-RL baselines (Search-R1, AutoRefine, IGPO) and their sparse-reward variants, and is competitive with much larger non-finetuned LLMs (GPT-5.2, DeepSeek-V4-Pro) under our diagnostic evaluation protocol. Relative to the strongest sparse-reward variant AutoRefine-HardSearch, C-MIG improves the average score by 9.30 (59.92 v.s. 50.62) on MedDDx-Plus, and by 1.20 (10.85 v.s. 9.65), 0.28 (9.71 v.s. 9.43), and 0.94 (18.38 v.s. 17.44) on the three out-of-domain datasets, respectively. In contrast to hard process

¹<https://developers.openai.com/api/docs/models/gpt-5.2>

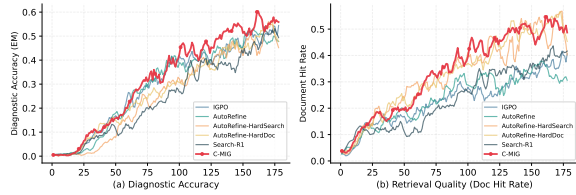


Figure 3: Training dynamics of (a) diagnostic accuracy and (b) document hit rate. Backbone: Qwen2.5-3B.

signal methods, C-MIG assesses process quality by measuring the change in the frozen reference model’s posterior probability of the ground-truth diagnosis, which effectively guides process improvement while avoiding the failure of hard signals in low-hit-rate clinical diagnosis scenarios.

Models trained with EM rewards exhibit a tendency to overfit the diagnostic expression patterns of the in-domain data. For instance, Search-R1 attains an average score of 55.98 on the in-domain MedDDx-Plus set, yet only 1.41 on the out-of-domain MedXpertQA set, demonstrating that exclusive reliance on EM rewards incurs substantial overfitting. In contrast, AutoRefine and IGPO, which incorporate refinement steps and process signals, achieve improved performance on OOD datasets.

Soft-reward methods generally achieve superior performance compared to hard-reward methods. Hard-reward approaches, which assign rewards based on whether the retrieved query or retrieved document contains the ground-truth diagnosis, inevitably encounter low hit rates for the ground-truth diagnosis in real-world clinical diagnosis scenarios, largely due to the inherent semantic similarity among medical diagnostic terminologies. By adopting a multi-view information-gain-based reward allocation mechanism, C-MIG achieves state-of-the-art performance, further demonstrating its effectiveness in the clinical consultation domain.

3.2.2 Consistency Analysis of Retrieval Quality and Diagnostic Accuracy

We further evaluate the enhancement of reasoning process capability afforded by C-MIG along two dimensions: diagnostic accuracy and document hit rate.

As shown in Figure 3, the diagnostic accuracy curve of C-MIG exhibits a steady upward trend throughout the entire training process. In contrast, AutoRefine plateaus or even fluctuates downward in the later training stages, suggesting that methods

Methods	Pearson r	DA	Doc Hit
Search-R1	0.988	0.513	0.403
AutoRefine	0.971	0.480	0.312
IGPO	0.963	0.522	0.375
AutoRefine-HardSearch	0.966	0.519	0.511
AutoRefine-HardDoc	0.991	0.518	0.515
C-MIG	0.994	0.558	0.508

Table 2: Pearson correlation (r) between diagnostic accuracy and document hit rate during training, alongside final diagnostic accuracy (DA) and document hit rate (Doc Hit).

lacking process-level rewards offer limited room for improvement in the clinical diagnosis scenario.

We further compute the Pearson correlation coefficient between diagnostic accuracy and document hit rate. As reported in Table 2, C-MIG achieves a Pearson correlation coefficient of $r = 0.994$, substantially higher than that of IGPO ($r = 0.963$) and AutoRefine-HardSearch ($r = 0.966$). This finding indicates that the process reward of C-MIG effectively aligns intermediate retrieval behavior with the ultimate diagnostic objective, such that each improvement in retrieval quality translates directly into a synchronous gain in diagnostic accuracy.

Notably, although AutoRefine-HardDoc achieves the highest document hit rate (0.515), its diagnostic accuracy (0.518) is substantially lower than C-MIG (0.558). This suggests that direct binary retrieval supervision encourages shortcut patterns that maximize ground-truth inclusion without developing robust reasoning, whereas the posterior-based indirect signal of C-MIG guides high-quality retrieval while preserving exploration. A detailed training stability analysis is provided in Appendix D.

3.2.3 Information Gain Analysis of the Reference Model and Policy Model

To validate the effectiveness of computing information gain via a reference model in C-MIG, we evaluate two alternative posterior computation schemes: (1) Ref, a frozen base model that shares the same architecture as the policy model; and (2) Policy, the continuously updated policy model itself. Table 3 reports the diagnostic average score achieved by the C-MIG-R process reward under these two posterior model configurations.

More detailed experimental results are presented in Appendix E. We draw the following conclusions:

Computing information gain via a frozen ref-

Methods	MD	MQA	MX	RJUA	Overall
Qwen2.5-3B					
Policy	46.36	8.85	8.23	21.61	21.26
Ref	56.75	9.05	7.03	19.43	23.07
Qwen2.5-7B					
Policy	59.23	17.75	3.84	17.54	24.59
Ref	62.59	16.75	8.78	19.10	26.81
Qwen2.5-3B-Instruct					
Policy	26.32	4.35	5.96	5.96	10.65
Ref	52.38	9.05	6.08	19.00	21.63
Qwen2.5-7B-Instruct					
Policy	54.32	16.95	9.16	16.44	24.22
Ref	57.50	17.15	7.36	19.38	25.35

Table 3: Analysis of posterior probability model selection. MD: MedDDx-Plus; MQA: MedQA, MX: MedXpertQA.

erence model alleviates reward drift. Regardless of model type or parameter size, using the policy model for posterior computation consistently yields lower diagnostic accuracy than the reference model. The continuously updated policy parameters cause identical documents to produce varying probability distributions across training stages, whereas the frozen reference model provides stable reward signals throughout training.

Larger model can mitigate the instability induced by the policy model. For the Qwen2.5-3B-Instruct, policy model leads to a 50.76%(10.65 v.s. 21.63) drop in overall performance relative to using the reference model, whereas the corresponding drop for the Qwen2.5-7B-Instruct model is only 4.45%(24.22 v.s. 25.35). This discrepancy indicates that increasing the model capacity enhances its robustness against the reward drift induced by the policy model. Moreover, the frozen reference model introduces only 3.4% computational overhead per training step (detailed in Appendix H).

3.2.4 Analysis of Rollout-Level Reward and Turn-Level Token Reward

While IGPO employs turn-level information gain as a local reward for tokens within each reasoning turn, C-MIG applies process rewards at the sequence level across entire trajectories. As both compute rewards from inter-turn differentials, we compare whether such signals should be assigned per-turn or aggregated into sequence-level rewards. We evaluate both granularities on IGPO and C-MIG-D using Qwen2.5-3B. Results

Granularity	MD	MQA	MX	RJUA	Overall
IGPO					
Turn	53.21	10.05	5.62	17.25	21.53
Seq	56.62	10.55	5.66	16.63	22.37
C-MIG-D					
Turn	51.50	9.30	8.82	19.62	22.31
Seq	57.55	10.10	9.32	17.39	23.59

Table 4: Comparative analysis of reward granularity. Turn: Turn-level, Seq: Sequence-level.

are shown in Table 4 (details in Appendix F).

Sequence-level approaches consistently outperform turn-level ones, yielding stable improvements particularly on MedDDx. In clinical knowledge bases, the relevance distribution between documents and diagnoses is highly dispersed, such that per-step information gain is both small in magnitude and large in variance. Directly utilizing such high-variance signals as token-level rewards injects noise into advantage estimation. In contrast, sequence-level methods aggregate signals across multiple retrieval rounds into a more stable trajectory-level advantage estimate, exhibiting stronger robustness in medical scenarios.

3.2.5 Scalability Analysis of Multi-View Information Gain

Methods	MD	MQA	MX	RJUA	Overall
AutoRefine-ICDTree	53.98	7.80	7.40	17.68	21.72
w/ $\Delta(s_{Refine})$	60.69	9.30	5.86	16.59	23.11
w/ $\Delta(s_{Doc})$	59.06	9.85	10.50	15.64	23.76

Table 5: Scalability of multi-view information gain based on AutoRefine-ICDTree.

To assess the scalability of multi-view information gain, we augment AutoRefine-ICDTree with information gain at the retrieval-document and document-refinement levels. Table 5 presents the results on Qwen2.5-3B as backbone.

Compared with AutoRefine-ICDTree, introducing information gain-based soft process rewards at the retrieval-document and document-refinement levels yields overall performance gains of 2.04 and 1.39, respectively, validating the scalability of our multi-view information gain mechanism. Full results across Qwen2.5-3B/7B (Base/Instruct) are in Appendix G.

3.3 Ablation Study

To validate the effectiveness of each component, we adopt Qwen2.5-3B as the base model and

Methods	MD	MQA	MX	RJUA	Overall
Base	50.06	9.50	6.23	16.44	20.56
w/ Doc	57.55	10.10	9.32	17.39	23.59
w/ Refine	56.75	9.05	7.03	19.43	23.07
w/ Subquery	58.09	10.80	2.18	15.83	21.73
C-MIG	59.92	10.85	9.71	18.38	24.72

Table 6: Ablation study by progressively adding components to the AutoRefineBase model.

progressively incorporate modules on top of AutoRefine: (1) w/ Doc, adding information gain from retrieved documents; (2) w/ Refine, adding information gain from refined content; and (3) w/ Subquery, adding the multi-subquery strategy. The full C-MIG integrates all three components. Results are presented in Table 6; detailed results with Qwen2.5-3B(instruct) and Qwen2.5-7B(base/instruct) backbones are in Appendix I. We draw the following conclusions:

The addition of each component improves overall performance, validating the effectiveness of our multi-view information gain mechanism and multi-subquery strategy. The gains from multi-view information gain are particularly substantial: w Doc and w Refine yield improvements of 3.03 and 2.51, respectively. Computing information gain from retrieved documents enhances retrieval quality, whereas computing it from refined content improves knowledge summarization capability. Together, they supervise two orthogonal capability dimensions: “retrieval planning” and “knowledge digestion.” Furthermore, the multi-subquery strategy transforms ambiguous patient descriptions into precise symptom queries, facilitating diagnostic performance. A case study is presented in Appendix J.

4 Related Work

RAG and Reinforcement Learning. Early RAG systems employ single-round retrieval with inherent limitations (Xiong et al., 2024). Recent works integrate RAG with RL for multi-round retrieval and reasoning (Li et al., 2025c; Song et al., 2025; Shi et al., 2026): ReSearch (Chen et al., 2025a) embeds search into reasoning chains, s3 (Wang et al., 2025b) decouples the searcher from the generator, MMOA-RAG (Chen et al., 2025c) formulates RAG modules as cooperative multi-agents, and DynamicRAG (Xu et al., 2025a) trains a reranker with generation-quality feedback. These methods either optimize a single module or lack fine-grained credit

assignment to intermediate steps—a gap C-MIG fills via multi-view information gain.

Process Reward for Multi-Turn Reasoning. Outcome-only rewards suffer from credit assignment in multi-step reasoning. Wang et al. (2025a) proposes information gain turn-level rewards using the policy model’s log-probability; Wang et al. (2026b) trains a process reward model via MCTS; Li et al. (2025d) uses LLM-judged document relevance; Zhao et al. (2025) eliminates policy bias through cross-family generation; Xiong et al. (2025) shows process DPO outperforms PPO/SFT. More recently, ReasonRAG (Ye et al., 2025) provides fine-grained rewards per RAG stage, LeTS (Chen et al., 2025b) hybridizes process and outcome rewards, HiPRAG (Zhang et al., 2026) introduces hierarchical rewards for search decisions, and Setlur et al. (2025) formalizes process reward as progress in success probability. Most methods require a trained reward model or LLM judge; C-MIG derives drift-resistant rewards from a frozen reference model without additional training.

Clinical RAG. LLM reasoning has extended to complex clinical diagnosis (Ma et al., 2026; Peng et al., 2025; Xia et al., 2025). MedRAG (Xu et al., 2025b) fuses diagnostic KGs with EHRs, MedGraphRAG (Wu et al., 2025) builds medical graph structures for evidence-based generation, and RAG² (Li et al., 2025a) filters retrieved passages via rationale models. For medical RAG-RL, Zheng et al. (2025) trains an agentic diagnostic system with a threefold RL framework, and Lu et al. (2025) designs multi-dimensional medical rewards covering entity coverage and KG path alignment. Existing clinical methods rely on exact-match or KG-alignment rewards that produce zero signal for semantically relevant outputs; C-MIG provides continuous information gain rewards suited to the naming ambiguity inherent in clinical diagnosis.

5 Conclusion

We propose **C-MIG**, a multi-view information gain-based retrieval-augmented generation for clinical diagnosis reasoning. Specifically, we introduce a multi-view information gain mechanism that derives reward signals from two complementary perspectives, the retrieved document level and the document refinement level, alleviating the issues of valuable reward signal loss and credit assignment. We further design a multi-subquery retrieval aug-

mentation strategy that improves knowledge recall coverage in clinical diagnostic scenarios. Extensive experiments on four medical evaluation benchmarks demonstrate that C-MIG achieves state-of-the-art performance, offering a reliable RAG-RL solution for clinical diagnosis.

Limitations

This work is subject to several limitations. Our method relies on a frozen reference model, the evaluation is restricted to text-only medical question answering and diagnostic dialogues without incorporating multi-modal evidence such as medical images, and the benchmarks used may not fully reflect the diversity of patient populations across different regions, languages, and healthcare systems. Accordingly, the experimental results presented in this paper should be interpreted as methodological evidence for the effectiveness of retrieval-augmented diagnostic reasoning, rather than as evidence of readiness for clinical deployment. All public models and baselines used in this work are employed under their original licenses or service terms, while proprietary large language models are accessed through their official services. Future work will focus on scaling C-MIG to larger and multi-modal foundation models, conducting broader cross-institutional and cross-lingual validation, and incorporating evaluations by professional clinicians together with safer evaluation protocols.

References

- Baichuan. 2023. [Baichuan 2: Open large-scale language models](#). *arXiv preprint arXiv:2309.10305*.
- Junyong Chen, Xidong Wang, Anningzhe Gao, Feng Jiang, Shunian Chen, Hongbo Zhang, Dingjie Song, Wenya Xie, Chuyi Kong, Jianquan Li, Xiang Wan, Haizhou Li, and Benyou Wang. 2023. [Huatuogpt-ii, one-stage training for medical adaption of llms](#). *Preprint*, arXiv:2311.09774.
- Mingyang Chen and 1 others. 2025a. Research: Learning to reason with search for llms via reinforcement learning. In *Advances in Neural Information Processing Systems (NeurIPS)*.
- Qiang Chen and 1 others. 2025b. Lets: Learning to think-and-search via process-and-outcome reward hybridization. In *Proceedings of the 2025 Conference on Empirical Methods in Natural Language Processing (EMNLP)*.
- Yiqun Chen and 1 others. 2025c. Improving retrieval-augmented generation through multi-agent reinforcement learning. In *Advances in Neural Information Processing Systems (NeurIPS)*.
- Clément Christophe, Praveen K Kanithi, Tathagata Raha, Shadab Khan, and Marco AF Pimentel. 2024. Med42-v2: A suite of clinical llms. *arXiv preprint arXiv:2408.06142*.
- DeepSeek-AI. 2026. Deepseek-v4: Towards highly efficient million-token context intelligence.
- Chengfeng Dou, Chong Liu, Fan Yang, Fei Li, Jiyuan Jia, Mingyang Chen, Qiang Ju, Shuai Wang, Shunya Dang, Tianpeng Li, and 1 others. 2025. Baichuanm2: Scaling medical capability with large verifier system. *arXiv preprint arXiv:2509.02208*.
- Arsene Fansi Tchango, Rishab Goel, Zhi Wen, Julien Martel, and Joumana Ghosn. 2022. Ddxplus: A new dataset for automatic medical diagnosis. *Advances in neural information processing systems*, 35:31306–31318.
- Yifan Feng, Hao Hu, Shihui Ying, Xingliang Hou, Shiquan Liu, Mingyuan Yang, Junchang Li, Shaoyi Du, Nanning Zheng, Han Hu, and 1 others. 2026. Hyper-rag: Combating llm hallucinations using hypergraph-driven retrieval-augmented generation. *Nature Communications*.
- Yu Gu, Robert Tinn, Hao Cheng, Michael Lucas, Naoto Usuyama, Xiaodong Liu, Tristan Naumann, Jianfeng Gao, and Hoifung Poon. 2021. Domain-specific language model pretraining for biomedical natural language processing. *ACM Transactions on Computing for Healthcare (HEALTH)*, 3(1):1–23.
- Daya Guo, Dejian Yang, Haowei Zhang, Junxiao Song, Peiyi Wang, Qihao Zhu, Runxin Xu, Ruoyu Zhang, Shirong Ma, Xiao Bi, and 1 others. 2025. Deepseek-r1: Incentivizing reasoning capability in llms via reinforcement learning. *arXiv preprint arXiv:2501.12948*.
- Lei Huang, Weijiang Yu, Weitao Ma, Weihong Zhong, Zhangyin Feng, Haotian Wang, Qianglong Chen, Weihua Peng, Xiaocheng Feng, Bing Qin, and 1 others. 2025. A survey on hallucination in large language models: Principles, taxonomy, challenges, and open questions. *ACM Transactions on Information Systems*, 43(2):1–55.
- Bowen Jin, Hansi Zeng, Zhenrui Yue, Jinsung Yoon, Sercan Arik, Dong Wang, Hamed Zamani, and Jiawei Han. 2025. Search-r1: Training llms to reason and leverage search engines with reinforcement learning. *arXiv preprint arXiv:2503.09516*.
- Di Jin, Eileen Pan, Nassim Oufattole, Wei-Hung Weng, Hanyi Fang, and Peter Szolovits. 2020. What disease does this patient have? a large-scale open domain question answering dataset from medical exams. *arXiv preprint arXiv:2009.13081*.
- Diederik P. Kingma and Jimmy Ba. 2015. Adam: A method for stochastic optimization. In *International Conference on Learning Representations (ICLR)*.

- Jiwoong Li and 1 others. 2025a. Rationale-guided retrieval augmented generation for medical question answering. In *Proceedings of the 2025 Conference of the North American Chapter of the Association for Computational Linguistics (NAACL)*.
- Siran Li, Linus Stenzel, Carsten Eickhoff, and Seyed Ali Bahrainian. 2025b. Enhancing retrieval-augmented generation: a study of best practices. In *Proceedings of the 31st International Conference on Computational Linguistics*, pages 6705–6717.
- Weitao Li, Boran Xiang, Xiaolong Wang, Zhinan Gou, Weizhi Ma, and Yang Liu. 2025c. Ur²: Unify RAG and reasoning through reinforcement learning. *arXiv preprint arXiv:2508.06165*.
- Yuan Li, Qi Luo, Xiaonan Li, Bufan Li, Qinyuan Cheng, Bo Wang, Yining Zheng, Yuxin Wang, Zhangyue Yin, and Xipeng Qiu. 2025d. R3-rag: Learning step-by-step reasoning and retrieval for llms via reinforcement learning. *arXiv preprint arXiv:2505.23794*.
- Yusheng Liao, Chaoyi Wu, Junwei Liu, Shuyang Jiang, Pengcheng Qiu, Haowen Wang, Yun Yue, Shuai Zhen, Jian Wang, Qianrui Fan, and 1 others. 2025. Ehr-r1: A reasoning-enhanced foundational language model for electronic health record analysis. *arXiv preprint arXiv:2510.25628*.
- Keer Lu, Zheng Liang, Youquan Li, Jiejun Tan, Xili Wang, Da Pan, Shusen Zhang, Guosheng Dong, Bin Cui, Yunhuai Liu, and 1 others. 2025. Med-r³: Enhancing medical retrieval-augmented reasoning of llms via progressive reinforcement learning. *arXiv preprint arXiv:2507.23541*.
- Shiwei Lyu, Chenfei Chi, Hongbo Cai, Lei Shi, Xiaoyan Yang, Lei Liu, Xiang Chen, Deng Zhao, Zhiqiang Zhang, Xiangguo Lyu, Ming Zhang, Fangzhou Li, Xiaowei Ma, Yue Shen, Jinjie Gu, Wei Xue, and Yiran Huang. 2023. *Rjua-qa: A comprehensive qa dataset for urology*. *Preprint*, arXiv:2312.09785.
- Siqi Ma, Jiajie Huang, Fan Zhang, Jinlin Wu, Yue Shen, Guohui Fan, Zhu Zhang, and Zelin Zang. 2026. Medla: A logic-driven multi-agent framework for complex medical reasoning with large language models. In *Proceedings of the AAAI Conference on Artificial Intelligence*, volume 40, pages 845–853.
- Andreas Maercker, Chris R Brewin, Richard A Bryant, Marylene Cloitre, Geoffrey M Reed, Mark Van Ommeren, Asma Humayun, Lynne M Jones, Ashraf Kagee, Augusto E Llosa, and 1 others. 2013. Proposals for mental disorders specifically associated with stress in the international classification of diseases-11. *The Lancet*, 381(9878):1683–1685.
- Hadas Orgad, Michael Tokar, Zorik Gekhman, Roi Reichart, Idan Szpektor, Hadas Kotek, and Yonatan Belinkov. 2025. LLMs know more than they show: On the intrinsic representation of LLM hallucinations. In *International Conference on Learning Representations*, volume 2025, pages 66880–66913.
- Qi Peng, Jialin Cui, Jiayuan Xie, Yi Cai, and Qing Li. 2025. Tree-of-reasoning: Towards complex medical diagnosis via multi-agent reasoning with evidence tree. In *Proceedings of the 33rd ACM International Conference on Multimedia*, pages 1744–1753.
- Pengcheng Qiu, Chaoyi Wu, Shuyu Liu, Yanjie Fan, Weiwei Zhao, Zhuoxia Chen, Hongfei Gu, Chuanjin Peng, Ya Zhang, Yanfeng Wang, and 1 others. 2025. Quantifying the reasoning abilities of llms on clinical cases. *Nature Communications*, 16(1):9799.
- Qwen, :, An Yang, Baosong Yang, Beichen Zhang, Binyuan Hui, Bo Zheng, Bowen Yu, Chengyuan Li, Dayiheng Liu, Fei Huang, Haoran Wei, Huan Lin, Jian Yang, Jianhong Tu, Jianwei Zhang, Jianxin Yang, Jiayi Yang, Jingren Zhou, and 25 others. 2025. *Qwen2.5 technical report*. *Preprint*, arXiv:2412.15115.
- Stephen E. Robertson and Steve Walker. 1994. Some simple effective approximations to the 2-Poisson model for probabilistic weighted retrieval. In *Proceedings of the 17th Annual International ACM SIGIR Conference on Research and Development in Information Retrieval (SIGIR '94)*, pages 232–241, London, UK. Springer-Verlag.
- Amrith Setlur and 1 others. 2025. Rewarding progress: Scaling automated process verifiers for LLM reasoning. In *International Conference on Learning Representations (ICLR)*.
- Yaorui Shi, Sihang Li, Chang Wu, Zhiyuan Liu, Junfeng Fang, Hengxing Cai, An Zhang, and Xiang Wang. 2026. Search and refine during think: Facilitating knowledge refinement for improved retrieval-augmented reasoning. *Advances in Neural Information Processing Systems*, 38:155930–155958.
- Huatong Song, Jinhao Jiang, Yingqian Min, Jie Chen, Zhipeng Chen, Wayne Xin Zhao, Lei Fang, and Jirong Wen. 2025. R1-searcher: Incentivizing the search capability in llms via reinforcement learning. *arXiv preprint arXiv:2503.05592*.
- Guoqing Wang, Sunhao Dai, Guangze Ye, Zeyu Gan, Wei Yao, Yong Deng, Xiaofeng Wu, and Zhenzhe Ying. 2025a. Information gain-based policy optimization: A simple and effective approach for multi-turn LLM agents. *arXiv preprint arXiv:2510.14967*.
- Liang Wang, Haonan Chen, Nan Yang, Xiaolong Huang, Zhicheng Dou, and Furu Wei. 2026a. Chain-of-retrieval augmented generation. *Advances in Neural Information Processing Systems*, 38:59888–59915.
- Zhao Wang, Ziliang Zhao, and Zhicheng Dou. 2026b. Prorag: Process-supervised reinforcement learning for retrieval-augmented generation. *arXiv preprint arXiv:2601.21912*.
- Zhuokai Wang and 1 others. 2025b. s3: You don't need that much data to train a search agent via RL. In *Proceedings of the 2025 Conference on Empirical Methods in Natural Language Processing (EMNLP)*.

- Junde Wu and 1 others. 2025. Medical graph rag: Evidence-based medical large language model via graph retrieval-augmented generation. In *Proceedings of the 63rd Annual Meeting of the Association for Computational Linguistics (ACL)*.
- Peng Xia, Jinglu Wang, Yibo Peng, Kaide Zeng, Zihan Dong, Xian Wu, Xiangru Tang, Hongtu Zhu, Yun Li, Linjun Zhang, and 1 others. 2025. Mmedagent-rl: Optimizing multi-agent collaboration for multimodal medical reasoning. *arXiv preprint arXiv:2506.00555*.
- Guangzhi Xiong, Qiao Jin, Zhiyong Lu, and Aidong Zhang. 2024. [Benchmarking retrieval-augmented generation for medicine](#). In *Findings of the Association for Computational Linguistics, ACL 2024*, Findings of ACL, pages 6233–6251. Association for Computational Linguistics.
- Guangzhi Xiong, Qiao Jin, Xiao Wang, Yin Fang, Haolin Liu, Yifan Yang, Fangyuan Chen, Zhixing Song, Dengyu Wang, Minjia Zhang, and 1 others. 2025. Rag-gym: Systematic optimization of language agents for retrieval-augmented generation. *arXiv preprint arXiv:2502.13957*.
- Jiashuo Xu and 1 others. 2025a. Dynamicrag: Leveraging outputs of large language model as feedback for dynamic reranking in retrieval-augmented generation. In *Advances in Neural Information Processing Systems (NeurIPS)*.
- Xuejiao Xu and 1 others. 2025b. Medrag: Enhancing retrieval-augmented generation with knowledge graph-elicited reasoning for healthcare copilot. In *Proceedings of the ACM Web Conference (WWW)*.
- Jingyu Ye and 1 others. 2025. Process vs. outcome reward: Which is better for agentic rag reinforcement learning. In *Advances in Neural Information Processing Systems (NeurIPS)*.
- Xuan Zhang and 1 others. 2026. Hiprag: Hierarchical process rewards for efficient agentic retrieval augmented generation. In *International Conference on Learning Representations (ICLR)*.
- Qingfei Zhao, Ruobing Wang, Dingling Xu, Daren Zha, and Limin Liu. 2025. R-search: Empowering llm reasoning with search via multi-reward reinforcement learning. *arXiv preprint arXiv:2506.04185*.
- Qiaoyu Zheng, Yuze Sun, Chaoyi Wu, Weike Zhao, Pengcheng Qiu, Yongguo Yu, Kun Sun, Jian Zhang, Yanfeng Wang, Ya Zhang, and 1 others. 2025. End-to-end agentic rag system training for traceable diagnostic reasoning. *arXiv preprint arXiv:2508.15746*.
- Yuxin Zuo, Shang Qu, Yifei Li, Zhangren Chen, Xuekai Zhu, Ermo Hua, Kaiyan Zhang, Ning Ding, and Bowen Zhou. 2025. Medxpertqa: Benchmarking expert-level medical reasoning and understanding. *arXiv preprint arXiv:2501.18362*.

A Prompt

The prompt template used for rollout generation is given as follows:

Prompt Template for Rollout Generation

You are an expert physician skilled in clinical diagnosis with multi-turn search engine calling. To answer questions, you must first reason through the available information using `<think>` and `</think>`. If you identify missing knowledge, you may issue a search request using `<search>` query `</search>` – generate up to 3 focused sub-queries separated by ";". The retrieval system will provide you with the most relevant documents enclosed in `<evidence>` and `</evidence>`. After each search, you need to summarize and refine the existing documents in `<refine>` and `</refine>`. You may send multiple search requests if needed. Once you have sufficient information, provide a concise final answer using `<diagnosis>` and `</diagnosis>`.

Question: {question}

B Experiments Setting

B.1 Hyperparameter

Training is performed with the Adam optimizer (Kingma and Ba, 2015), using a learning rate of 6×10^{-7} , a batch size of 64. We sample a group of $G = 4$ rollouts with a maximum response length of 2,048 tokens. The clip ratio is set to 0.2, the KL regularization coefficient β to 0.001 for training stability.

Reward Weights. We set the format reward weight $w_f = 1$, diagnostic reward weight to 1 (exact match), and hard retrieval reward weight to 0.1. For the multi-turn retrieval information gain, we set weight $w_d = 1$ with sensitivity parameter $\alpha_d = 1$, and the refine reward weight $w_r = 0.1$. The elevated weight for information gain ($w_d = 1$) is motivated by the observation that in medical retrieval scenarios, reward signals are inherently sparse and models tend to collapse into single-turn retrieval without sufficient process-level supervision.

Non-linear Reward Composition. Following AutoRefine (Shi et al., 2026), we adopt a non-linear reward composition strategy rather than a simple linear summation. Specifically, when the diagnosis is correct, the total reward is computed as $R_{\text{total}} = R_{\text{format}} + R_{\text{diag}} + R_{\text{doc}}$, bypassing other process rewards to prevent over-crediting intermediate

steps when the final outcome is already successful. When the diagnosis is incorrect, the total reward reduces to $R_{\text{total}} = R_{\text{format}} + R_{\text{doc}} + R_{\text{refine}}$, providing process-level feedback to guide the model toward better retrieval and refinement behaviors. As demonstrated in Shi et al. (2026), a linear combination of answer and process rewards tends to over-emphasize intermediate behaviors, whereas the non-linear design prioritizes final answer correctness while still fostering robust retrieval and refinement capabilities.

Retrieval Configuration. For retrieval-augmented generation, we use the medical retrieval corpus from Zheng et al. (2025), which aggregates approximately 23.9M PubMed abstracts, 3.31M biomedical Wikipedia entries, 18 authoritative medical textbooks, and around 1,419 healthcare web resources (e.g., NCBI, NHS, Mayo Clinic, MedlinePlus, MSD Manuals), providing comprehensive clinical knowledge coverage. We employ BM25 (Robertson and Walker, 1994) as the retriever with a Top- k of 3 and allow up to $T_{\text{max}} = 3$ retrieval turns per response. All experiments are conducted on 4 H800 GPUs.

B.2 Train and Test Datasets

We use MedDDx-Plus (Fanshi Tchango et al., 2022) as the training dataset, which covers clinical diagnostic scenarios across multiple specialties, with each sample consisting of a patient symptom description and its corresponding standard diagnostic label. We uniformly sample 8,998 instances for training and 1,003 instances for validation from the original dataset.

To comprehensively evaluate the generalization capability of the model, we conduct evaluations on one in-domain (ID) dataset and three out-of-domain (OOD) datasets. The in-domain evaluation is performed on **MedDDx-Plus**, whose test subset is drawn from the same source as the training set and contains 1,003 evaluation instances. Since the original OOD benchmarks are in multiple-choice or non-English formats, we employ GPT-5.2 to pre-process them into a unified open-ended English QA format suitable for diagnostic evaluation. The three OOD datasets are: (1) **MedQA** (Jin et al., 2020), originally a multiple-choice medical examination benchmark containing many pharmacology-related questions; we use GPT-5.2 to filter instances suitable for disease diagnosis and convert them from multiple-choice to open-ended QA format, yield-

Methods	MedDDx-Plus			MedQA			MedXpertQA			RJUA			Overall Avg
	EM	KG	Avg	EM	KG	Avg	EM	KG	Avg	EM	KG	Avg	
Base model Qwen2.5-7B	2.99	5.80	4.39	0.00	2.90	1.45	0.59	2.65	1.68	0.00	0.76	0.38	1.98
RAG+RL Methods													
Search-RL	55.43	58.82	57.12	11.00	20.80	15.90	3.76	5.98	4.87	10.43	20.47	15.45	23.33
AutoRefine	53.94	56.49	55.22	12.00	19.80	15.90	4.55	7.41	5.98	10.43	25.21	17.82	23.73
IGPO	52.84	56.21	54.53	13.00	22.60	17.80	3.76	7.22	5.74	8.53	28.63	18.58	24.16
Clinical Sparse Reward Methods													
AutoRefine-Embedding	58.03	63.19	60.61	13.50	22.10	17.80	3.76	6.77	5.26	9.48	24.83	17.16	25.20
AutoRefine-ICDTree	47.16	60.92	54.04	11.00	23.70	17.35	5.15	8.91	7.03	9.00	21.71	15.36	23.44
AutoRefine-HardSearch	58.62	63.51	61.06	10.50	23.40	16.95	5.15	11.17	8.16	9.48	23.51	16.50	25.66
AutoRefine-HardDoc	57.03	60.82	58.92	10.50	20.20	15.35	7.13	12.95	10.04	10.90	25.88	18.39	25.67
C-MIG	60.82	65.12	62.97	11.00	20.40	15.70	7.52	13.39	10.46	11.37	27.49	19.43	27.14

Table 7: Performance on the in-domain dataset MedDDx-Plus and three out-of-domain datasets: MedQA, MedXpertQA, RJUA. Backbone: Qwen2.5-7B.

ing 200 instances; (2) **MedXpertQA** (Zuo et al., 2025), an expert-level multiple-choice medical dataset of 505 instances comprising challenging interdisciplinary diagnostic questions, converted to QA format via GPT-5.2; and (3) **RJUA** (Lyu et al., 2023), a real-world Chinese urology consultation dialogue dataset of 211 instances, characterized by highly colloquial patient descriptions and frequent multi-disease co-diagnosis, which we translate into professional English format using GPT-5.2.

B.3 Evaluation Metrics

Outcome Metrics. In our setting each model outputs a single diagnosis per case. We adopt two diagnostic accuracy metrics with complementary granularity:

- **Exact Match (EM).** Returns 1 if the normalized prediction exactly matches the ground truth after lowercasing and punctuation removal. EM reflects the strictest diagnostic correctness criterion.
- **Knowledge Graph Score (KG).** A continuous metric based on ICD-10 tree distance:

$$KG = \max(0, 1 - \alpha \cdot d(\hat{c}, c^*)), \quad \alpha = 0.2 \quad (11)$$

where $d(\hat{c}, c^*)$ is the shortest path length between the predicted and ground-truth ICD-10 codes through their Lowest Common Ancestor. Free-text diagnoses are mapped to ICD-10 codes via a cascaded strategy: regex extraction of explicit codes, exact dictionary lookup with inverted-index scoring over WHO ICD-10 descriptions, and an LLM fallback for unresolved cases; failed mappings receive a score of 0. KG rewards correct disease-family identification while remaining agnostic to within-

category severity differences—a deliberate design choice complemented by strict EM evaluation.

- **Embedding Similarity (Emb).** We compute the cosine similarity between diagnosis embeddings obtained from PubMedBERT (Gu et al., 2021), with a threshold $\tau = 0.6$ to suppress spurious matches:

$$\text{Emb} = \begin{cases} \cos(f(\hat{y}), f(y)) & \text{if } \cos(\cdot) \geq \tau \\ 0 & \text{otherwise} \end{cases} \quad (12)$$

We report EM and KG as the primary evaluation metrics across all methods. Embedding similarity, while useful as a soft training reward (AutoRefine-Embedding), is not used for evaluation, because embedding-based scores lack interpretable clinical semantics: a high cosine similarity does not guarantee diagnostic equivalence, whereas ICD-10 tree distance directly reflects taxonomic proximity in the standardized medical coding system. Together, EM ensures precision while KG captures clinically meaningful partial correctness.

Process Reward Baselines. We implement hard process reward variants upon AutoRefine (Shi et al., 2026). Given the gold answer $a = (a_1, \dots, a_L)$ of length L , all variants share a unified binary form:

$$R_{\text{process}} = \mathbb{I}[a \subseteq \mathcal{I}_t] \quad (13)$$

where \mathbb{I} denotes the binary indicator operator that takes the value of either 0 or 1 and \mathcal{I}_t denotes the intermediate content at turn t . Depending on the variant, \mathcal{I}_t corresponds to: the refined knowledge summary (AutoRefine base), the generated

search query (AutoRefine-HardSearch), or the retrieved documents (AutoRefine-HardDoc). These binary signals suffer from the same sparsity as EM: they cannot distinguish near-miss from irrelevant results.

Document Hit (Doc_Hit). We use Doc_Hit as the retrieval quality evaluation metric, defined identically to AutoRefine-HardDoc but aggregated over all turns:

$$\text{Doc_Hit} = \mathbb{I} \left[a \subseteq \bigcup_{t=1}^T \mathcal{D}_t \right] \quad (14)$$

This metric measures whether the model successfully retrieves diagnostically relevant evidence across the entire reasoning process, serving as a necessary prerequisite for accurate diagnosis.

C Main Result on Qwen-2.5-7B

We additionally conduct experiments and evaluations using Qwen2.5-7B as backbones. The experimental results are shown in Table 7.

C-MIG achieves an overall average of 27.14 (24.72 on Qwen2.5-3B) across the four medical evaluation benchmarks, surpassing the strongest baseline AutoRefine-HardDoc by +1.47 and the competing RAG-RL method IGPO by +2.98. On MedDDx-Plus (in-domain), MedXpertQA, and RJUA datasets that are most aligned with realistic clinical diagnostic scenarios, C-MIG consistently attains the best performance, thereby demonstrating the effectiveness of the multi-view information gain reward together with the posterior probability signal derived from the frozen reference model in mitigating reward drift.

D Training Stability Analysis

We provide a comprehensive analysis of training stability metrics for all methods on Qwen2.5-3B, including sequence entropy, late-stage volatility, gradient norm, process reward dynamics, and response length.

D.1 Sequence Entropy

Figure 4(a) shows the entropy loss curves during training. The linear regression slope of entropy reflects the rate of output uncertainty growth, as shown in Table 8.

C-MIG’s entropy growth rate (0.0023) is lower than AutoRefine (0.0033) and AR-HardDoc (0.0029), demonstrating that multi-view information gain rewards effectively suppress uncontrolled

Method	Slope	R^2	Trend
Search-R1	-0.0008	0.03	Decrease
AutoRefine	0.0033	0.58	Unstable
IGPO	0.0019	0.38	Moderate
AutoRefine-HardSearch	0.0005	0.02	Stagnant
AutoRefine-HardDoc	0.0029	0.55	Faster
C-MIG	0.0023	0.54	Controlled

Table 8: Entropy trend analysis (linear fit slope). C-MIG maintains moderate growth, lower than AutoRefine and AutoRefine-HardDoc.

uncertainty expansion while improving diagnostic capability. AutoRefine-HardSearch exhibits near-zero entropy change (slope 0.0005, $R^2 = 0.02$), as the hard signal is almost always zero, suppressing the model’s exploration behavior.

D.2 Late-Stage Volatility

We compute the standard deviation of the last 30% of training steps as a volatility metric, as shown in Table 9.

Method	Diag. $\sigma \downarrow$	DocHit $\sigma \downarrow$
Search-R1	0.074	0.053
AutoRefine	0.054	0.055
IGPO	0.071	0.063
AutoRefine-HardSearch	0.067	0.112
AutoRefine-HardDoc	0.070	0.060
C-MIG	0.060	0.051

Table 9: Late-stage volatility (std of last 30% steps). C-MIG achieves the lowest combined volatility.

C-MIG exhibits the lowest or near-lowest late-stage volatility in both diagnostic accuracy and document hit rate. Notably, AutoRefine-HardSearch’s retrieval volatility (0.112) is $2.2\times$ that of C-MIG, indicating that hard process signals in clinical scenarios lead to extremely sparse rewards and consequent training instability.

D.3 Gradient Norm Stability

Method	Mean	Std	CV \downarrow
Search-R1	1.15	0.23	0.20
AutoRefine	0.77	0.11	0.14
IGPO	0.62	0.16	0.25
AutoRefine-HardSearch	0.59	0.13	0.22
AutoRefine-HardDoc	1.08	0.13	0.12
C-MIG	1.01	0.18	0.18

Table 10: Gradient norm statistics (last 30% steps). CV: coefficient of variation. IGPO’s highest CV reflects gradient noise from reward drift.

We compare the gradient norm stability across different models, as illustrated in Figure 4(b) and

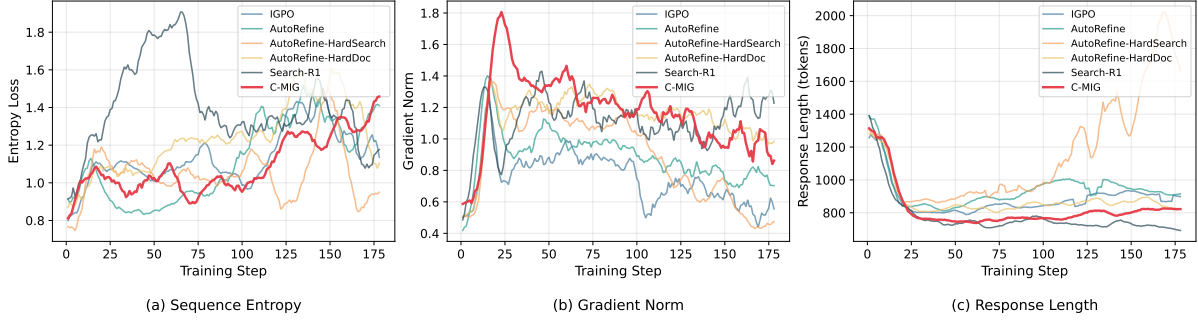


Figure 4: Training dynamics across all methods (after smoothing). (a) Sequence entropy. (b) Gradient norm. (c) Average response length.

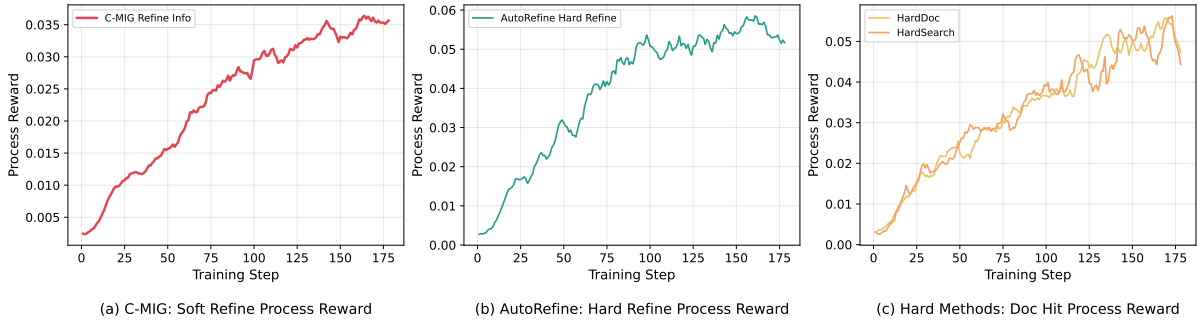


Figure 5: Process reward curves. (a) C-MIG soft refine information gain. (b) AutoRefine hard refine reward. (c) HardDoc/HardSearch document hit reward.

Table 10. C-MIG maintains a gradient norm mean of 1.012 (higher than IGPO’s 0.622, indicating sufficient learning signal) with a moderate CV of 0.181. IGPO exhibits the highest CV (0.250), confirming that computing information gain with the continuously updated policy model introduces gradient noise due to reward drift.

D.4 Process Reward Signal Analysis

Reward Type	Mean	Slope	$R^2 \uparrow$
HardDoc (hard)	0.033	2.8e-4	0.89
AutoRefine Hard Refine (hard)	0.039	3.0e-4	0.79
HardSearch (hard)	0.033	2.7e-4	0.77
C-MIG Refine (soft)	0.024	1.9e-4	0.91

Table 11: Process reward statistics. R^2 measures trend consistency.

Figure 5 and Table 11 present the process reward curves and the corresponding process reward statistics across different models, respectively. We can draw the three observations: (1) C-MIG’s soft process reward achieves the highest trend consistency ($R^2 = 0.91$), indicating a stable and predictable growth pattern that facilitates continuous learning. (2) Hard rewards have higher mean values but lower trend consistency, as their binary nature introduces stochastic fluctuations. (3) The gradual

growth pattern of soft rewards provides direction-consistent optimization gradients, whereas the binary nature of hard rewards leads to higher gradient variance.

D.5 Response Length

Figure 4(c) presents the response length curves. All methods exhibit a decreasing response length trend (from ~ 1400 to ~ 800 – 1100 tokens), indicating that models learn more concise reasoning expressions. C-MIG’s response length remains comparable to other methods, confirming that multi-view information gain rewards do not introduce redundant output.

E Information Gain Analysis of the Reference Model and Policy Model

Building upon Qwen2.5-3B (Base/Instruct) and Qwen2.5-7B (Base/Instruct) as backbone models, we systematically compare model performance under varying posterior probability configurations. The corresponding experimental results are summarized in Table 12. We can draw the following observations:

(1) w/ Ref consistently outperforms w/ Policy across all backbones, yielding overall average improvements ranging from +0.02 to +8.90,

Backbone	Methods	MedDDx-Plus			MedQA			MedXpertQA			RJUA			Overall Avg
		EM	KG	Avg	EM	KG	Avg	EM	KG	Avg	EM	KG	Avg	
Qwen2.5-3B	C-MIG-R w/ Policy	43.17	49.55	46.36	5.50	12.20	8.85	4.95	11.52	8.23	15.17	28.06	21.61	21.26
	C-MIG-R w/ Ref	55.03	58.46	56.75	5.50	12.60	9.05	4.36	9.70	7.03	11.85	27.01	19.43	23.07
	C-MIG-D w/ Policy	54.34	57.37	55.86	5.50	15.30	10.40	5.94	9.90	7.92	11.37	24.17	17.7	22.99
	C-MIG-D w/ Ref	56.43	58.6	57.55	7.00	13.20	10.10	6.93	11.72	9.32	9.00	25.78	17.39	23.59
Qwen2.5-3B-Instruct	C-MIG-R w/ Policy	22.23	30.41	26.32	1.50	7.20	4.35	3.37	8.55	5.96	3.37	8.55	5.96	10.65
	C-MIG-R w/ Ref	48.85	55.91	52.38	5.00	13.10	9.05	3.96	8.20	6.08	10.43	27.58	19.00	21.63
	C-MIG-D w/ Policy	25.92	28.22	27.07	5.00	12.60	8.80	3.17	8.59	5.88	10.43	27.58	19.00	15.19
	C-MIG-D w/ Ref	47.96	54.78	51.37	6.50	15.90	11.20	4.16	8.87	6.51	10.43	27.39	18.91	22.00
Qwen2.5-7B	C-MIG-R w/ Policy	57.13	61.32	59.23	11.50	24.00	17.75	2.77	4.91	3.84	9.95	25.12	17.54	24.59
	C-MIG-R w/ Ref	60.32	64.87	62.59	12.50	21.00	16.75	6.34	11.21	8.78	10.90	27.30	19.10	26.81
	C-MIG-D w/ Policy	44.37	51.74	48.05	15.50	25.00	20.25	7.52	12.99	10.25	7.52	12.99	10.25	22.20
	C-MIG-D w/ Ref	53.74	57.73	55.73	11.50	21.40	16.45	6.93	12.51	9.72	14.69	27.68	21.18	25.77
Qwen2.5-7B-Instruct	C-MIG-R w/ Policy	52.14	56.49	54.32	12.00	21.90	16.95	6.73	11.60	9.16	11.85	21.04	16.44	24.22
	C-MIG-R w/ Ref	55.13	59.88	57.50	12.00	22.30	17.15	5.54	9.19	7.36	13.74	25.02	19.38	25.35
	C-MIG-D w/ Policy	49.35	56.73	53.04	10.50	21.10	15.80	5.54	10.26	7.90	11.37	20.85	16.11	23.21
	C-MIG-D w/ Ref	50.55	54.34	52.44	9.00	16.00	12.50	6.14	10.81	8.48	9.95	20.19	15.07	22.12

Table 12: Performance comparison of C-MIG variants across in-domain (MedDDx-Plus) and out-of-domain (MedQA, MedXpertQA, RJUA) benchmarks.

Backbone	Methods	MedDDx-Plus			MedQA			MedXpertQA			RJUA			Overall Avg
		EM	KG	Avg	EM	KG	Avg	EM	KG	Avg	EM	KG	Avg	
Qwen2.5-3B	IGPO w/ Turn	51.84	54.58	53.21	7.00	13.10	9.30	4.55	6.69	5.62	8.53	25.97	17.25	21.53
	IGPO w/ Seq	55.03	58.21	56.62	6.50	14.60	10.55	4.16	7.17	5.66	9.95	23.32	16.63	22.37
	C-MIG-D w/ Turn	50.05	52.96	51.50	6.00	12.60	9.30	6.14	11.49	8.82	11.37	27.87	19.62	22.31
	C-MIG-D w/ Seq	56.43	58.66	57.55	7.00	13.20	10.10	6.93	11.72	9.32	9.00	25.78	17.39	23.59
Qwen2.5-7B	IGPO w/ Turn	52.84	56.21	54.53	13.00	22.60	17.80	3.76	7.22	5.74	8.53	28.63	18.58	24.16
	IGPO w/ Seq	52.94	52.18	52.56	12.50	22.70	17.60	5.74	10.50	8.12	11.37	26.64	19.00	24.32
	C-MIG-D w/ Turn	0.60	10.23	5.42	0.50	2.70	1.60	0.79	4.04	2.42	0.00	0.57	0.28	2.43
	C-MIG-D w/ Seq	53.74	57.73	55.73	11.50	21.40	16.45	6.93	12.51	9.72	14.69	27.68	21.18	25.77

Table 13: Comparison of granularity (*w/ Turn* vs. *w/ Seq*) for IGPO and C-MIG-D across in-domain (MedDDx-Plus) and out-of-domain (MedQA, MedXpertQA, RJUA) benchmarks.

which validates that the frozen reference model effectively mitigates reward drift. (2) the gain from Policy to Ref is particularly pronounced on smaller and instruction models (reaching +10.98 on Qwen2.5-3B-Instruct), indicating that the more severe the distributional shift during training, the more critical the stabilizing role of the reference model becomes.

F Analysis of Rollout-Level Reward and Turn-Level Token Reward

We additionally conduct analysis of rollout-level reward and turn-level token reward using Qwen2.5-3B(Base) and Qwen2.5-7B (Base) as backbones. The experimental results are shown in Table 13. Sequence-level rewards yield overall average gains

of +0.84 / +1.28 on Qwen2.5-3B and +0.16 / +23.34 on Qwen2.5-7B for IGPO and C-MIG-D respectively, indicating that aggregated trajectory-level signals provide a more stable optimization target than dense turn-level rewards.

G Scalability Analysis of Multi-View Information Gain

We conduct scalability experiments on multi-view information gain based on Qwen2.5-3B (Base/Instruct) and Qwen2.5-7B (Base/Instruct), respectively as backbone. The experimental results are shown in Table 14. We can draw the following conclusions:

(1) Across all four backbones, both $w/ \Delta(s_{\text{Refine}})$ and $w/ \Delta(s_{\text{Doc}})$ consistently outperform

Methods	MedDDx-Plus			MedQA			MedXpertQA			RJUA			Overall Avg
	EM	KG	Avg	EM	KG	Avg	EM	KG	Avg	EM	KG	Avg	
<i>Qwen2.5-3B</i>													
AutoRefine-ICDTree	43.87	64.09	53.98	3.00	12.60	7.80	4.95	9.86	7.40	9.00	26.30	17.68	21.72
w/ $\Delta(s_{Refine})$	52.54	68.85	60.69	5.50	13.10	9.30	3.76	7.96	5.86	10.90	22.27	16.59	23.11
w/ $\Delta(s_{Doc})$	51.25	66.86	59.06	5.50	14.20	9.85	7.92	13.07	10.50	8.06	23.22	15.64	23.76
<i>Qwen2.5-7B</i>													
AutoRefine-ICDTree	47.16	60.92	54.04	11.00	23.70	17.35	5.15	8.91	7.03	9.00	21.71	15.36	23.45
w/ $\Delta(s_{Refine})$	55.03	72.64	63.84	11.50	21.20	16.35	6.34	11.92	9.13	18.01	30.43	24.22	28.39
w/ $\Delta(s_{Doc})$	47.46	65.70	56.58	10.00	22.90	16.45	6.34	11.13	8.74	16.59	25.59	21.09	25.72
<i>Qwen2.5-3B-Instruct</i>													
AutoRefine-ICDTree	42.07	52.34	47.20	7.50	11.70	9.60	7.13	11.88	9.51	9.48	25.40	17.44	20.94
w/ $\Delta(s_{Refine})$	45.76	55.89	50.82	8.50	13.00	10.75	7.72	14.53	11.12	7.58	24.36	15.97	22.17
w/ $\Delta(s_{Doc})$	40.28	60.30	50.29	5.50	13.20	9.35	4.95	9.74	7.35	12.80	26.45	19.62	21.65
<i>Qwen2.5-7B-Instruct</i>													
AutoRefine-ICDTree	42.07	52.34	47.20	7.50	11.70	9.60	7.13	11.88	9.51	9.48	25.40	17.44	20.94
w/ $\Delta(s_{Refine})$	44.37	60.20	52.28	12.00	21.50	16.75	6.93	12.87	9.90	8.53	24.55	16.54	23.87
w/ $\Delta(s_{Doc})$	39.48	54.96	47.22	12.00	21.60	16.80	9.90	17.82	13.86	12.32	23.13	17.73	23.90

Table 14: Scalability of multi-view information gain based on AutoRefine-IDCTree across different model as backbone.

AutoRefine-ICDTree, yielding overall average improvements ranging from +0.71 to +4.94. This confirms the scalability and effectiveness of our proposed multi-view information gain. $(2)\Delta(s_{Refine})$ is preferred on larger and instruction-tuned backbones (e.g., +4.94 on Qwen2.5-7B), whereas $\Delta(s_{Doc})$ is more effective on smaller base models (+2.04 on Qwen2.5-3B). This indicates that higher-capacity policies benefit more from compressed, semantically-distilled views, while smaller models gain more from the richer signal preserved in raw documents.

H Computational Overhead Analysis

The information-theoretic reward signals require additional forward passes through a frozen reference model to compute $\text{LogitP}(a | \mathcal{I}_{\text{extra}}) - \text{LogitP}(a | \mathcal{I}_{\text{base}})$ (Eq. 2) during the reward assignment phase of each GRPO training step. We employ a persistent multi-GPU worker pool that maintains the reference model (Qwen2.5-3B, bfloat16) in GPU memory across all training steps, combined with dynamic token-budget batching that adaptively determines batch sizes based on actual sequence lengths to maximize GPU utilization.

We measure the computational overhead on $4 \times \text{H800}$ (80GB) GPUs over 180 training steps. The reference model occupies approximately 6.8 GB per GPU (<8.5% of H800 memory), co-existing with the actor model without memory contention. Computing both reward signals (refine-

ment information gain and per-turn information increase) adds only 3.14 seconds per step (2.81s + 0.33s), corresponding to a 3.4% overhead ratio relative to the total step time. The overall training wall-clock increases by less than 5% compared to the baseline without information-theoretic rewards (4.84h vs. 3.71h for 180 steps, where the gap is primarily attributable to longer rollout sequences encouraged by the retrieval reward rather than reward computation).

I Ablation Study

We conduct ablation study and evaluations using Qwen2.5-3B(Base) and Qwen2.5-7B (Base) as backbones. The experimental results are shown in Table 15.

Ablation studies demonstrate that both our proposed multi-view information gain mechanism and multi-subquery mechanism yield consistent improvements across diverse model, further substantiating the effectiveness of C-MIG.

J Case Study

We randomly select a sample from the test set for evaluation, and the result is illustrated in Figure 6. This case qualitatively demonstrates how the multi-subquery decomposition and multi-view information gain in C-MIG jointly enable robust diagnostic reasoning.

Backbone	Method	MedDDx-Plus			MedQA			MedXpertQA			RJUA			Overall Avg
		EM	KG	Avg	EM	KG	Avg	EM	KG	Avg	EM	KG	Avg	
Qwen2.5-3B	AutoRefineBase	48.65	51.47	50.06	7.00	12.00	9.50	3.96	8.51	6.23	8.53	24.35	16.44	20.56
	w/ Doc	56.43	58.66	57.55	7.00	13.20	10.10	6.93	11.72	9.32	9.00	25.78	17.39	23.59
	w/ Refine	55.03	58.46	56.75	5.50	12.60	9.05	4.36	9.70	7.03	11.85	27.01	19.43	23.07
	w/ Subquery	56.23	59.96	58.09	8.50	13.10	10.80	1.39	2.97	2.18	9.95	21.71	15.83	21.73
	C-MIG	57.43	62.41	59.92	6.50	15.20	10.85	7.33	12.08	9.71	9.95	26.83	18.38	24.72
Qwen2.5-7B	AutoRefineBase	53.94	56.49	55.22	12.00	19.80	15.90	4.55	7.41	5.98	10.43	25.21	17.82	23.73
	w/ Doc	53.74	57.73	55.73	11.50	21.40	16.45	6.93	12.51	9.72	14.69	27.68	21.18	25.77
	w/ Refine	60.32	64.87	62.59	12.50	21.00	16.75	6.34	11.21	8.78	10.90	27.30	19.10	26.81
	w/ Subquery	60.02	62.15	61.09	12.50	22.40	17.45	5.54	9.98	7.76	10.43	26.64	18.54	26.21
	C-MIG	60.82	65.12	62.97	11.00	20.40	15.70	7.52	13.39	10.46	11.37	27.49	19.43	27.14

Table 15: Ablation study of C-MIG components on in-domain (MedDDx-Plus) and out-of-domain (MedQA, MedXpertQA, RJUA) benchmarks.

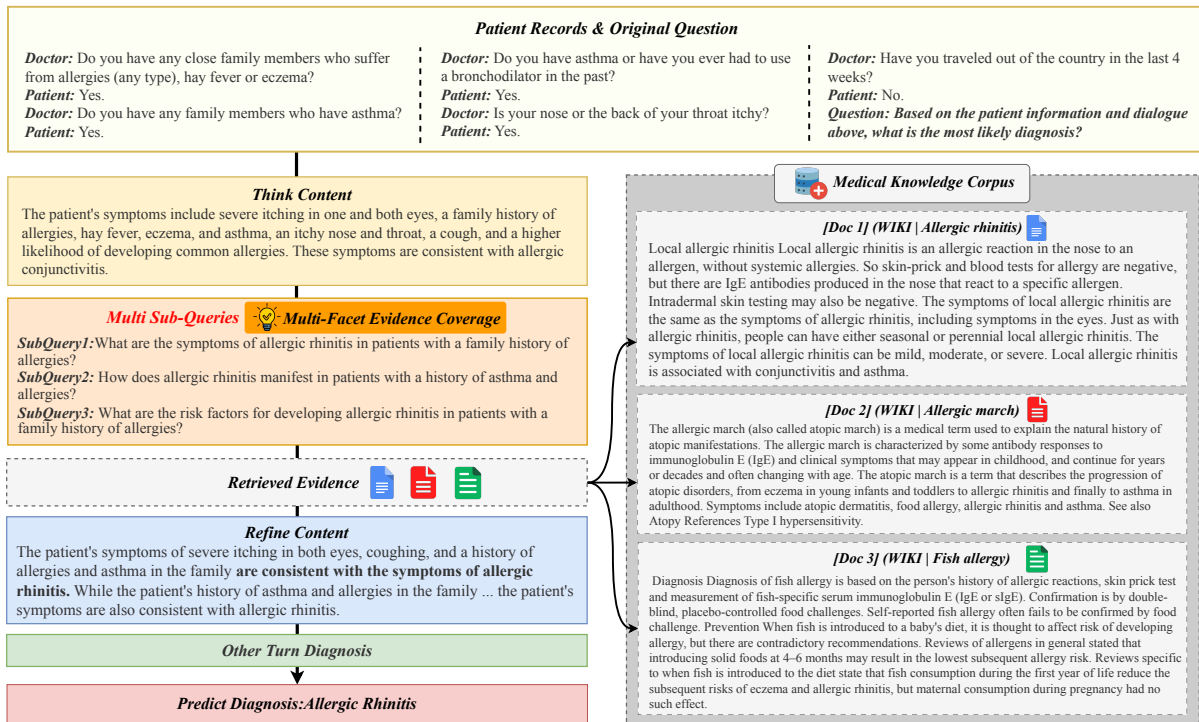


Figure 6: Case study. C-MIG performs step-by-step diagnostic reasoning.

Multi-Subquery Decomposition. Given a patient presenting with severe eye itching, family history of allergies/asthma, nasal itching, and cough, the model first generates a Think Content that summarizes key symptoms and forms an initial hypothesis (allergic conjunctivitis). It then decomposes the colloquial description into three complementary, medically standardized subqueries: (1) “What are the symptoms of allergic rhinitis in patients with a family history of allergies?” targeting symptom-disease mapping; (2) “How does allergic rhinitis manifest in patients with a history of asthma and allergies?” targeting comorbidity patterns; and (3) “What are the risk factors for developing allergic rhinitis in patients with a family history of allergies?” targeting epidemiological risk

factors. This decomposition ensures multi-facet evidence coverage: the three subqueries retrieve documents spanning disease definition (Allergic rhinitis), progression patterns (Allergic march), and differential factors (Fish allergy), providing complementary knowledge that a single query would fail to cover.

Information Gain-Guided Retrieval and Refinement Quality. The retrieved documents contain both highly relevant evidence. Under the C-MIG-D reward, the model is incentivized to retrieve documents that maximally increase $\text{LogitP}(a | q, D_k)$ relative to the previous turn, effectively filtering noise across rounds. In the Refine Content, the model synthesizes relevant evidence while discard-

ing irrelevant information (fish allergy), producing a concise summary: “the patient’s symptoms of severe itching in both eyes, coughing, and a history of allergies and asthma in the family **are consistent with the symptoms of allergic rhinitis.**” The C-MIG-R reward ensures that only refinements genuinely increasing diagnostic confidence (i.e., $\Delta(s_{\text{refine}}) > 0$) receive positive reward, guiding the model to extract diagnostically decisive content rather than passively paraphrasing retrieved documents. The model ultimately arrives at the correct diagnosis of Allergic Rhinitis through multi-turn reasoning.